Rapid Communications

Polymer in wedge-shaped confinement: Effect on the θ temperature

Sanjay Kumar,[1] Keerti Chauhan,[1] Sadhana Singh,[1] and Damien Foster[2]
[1]*Department of Physics, Banaras Hindu University, Varanasi 221005, India*
[2]*Centre for Data Science, Coventry University, Coventry CV1 5FB, United Kingdom*

(Received 13 August 2019; accepted 29 January 2020; published 20 March 2020)

The equilibrium properties of a finite-length linear polymer chain confined in an infinite wedge composed of two perfectly reflecting hard walls meeting at a variable apex angle (α) are presented. One end of the polymer is anchored a distance y from the apex on the conical axis of symmetry, while the other end is free. We report here, the nonmonotonic behavior of θ temperature as a function of y for a finite-length chain. Data collapse for different chain lengths indicates that such behavior will exist for all finite lengths. We delineate the origin of such nonmonotonic behavior, which may have potential applications in understanding the cellular process occurring in nanoconfined geometries.

DOI: 10.1103/PhysRevE.101.030502

Living organisms maintain homeostasis, and therefore, most cellular processes occur at roughly constant temperature [1]. Efforts have been made to understand such processes *in vivo* by analyzing them *in vitro* [2–4]. For example, melting of DNA [5], unfolding of protein [6,7], DNA unzipping [8–11], DNA denaturation [12], coil-globule transition of polymers [13], and translocation [14] are a few examples, where a good understanding about the process has been achieved. However, *in vivo* the surrounding environment does not change as drastically as it has typically been changed during *in vitro* experiments. For example, DNA melting occurs at $85 \pm 5\,^{\circ}$C, whereas normal body temperature remains at $37 \pm 2\,^{\circ}$C [12]. Therefore, there is a need for another route similar to the cell, where a slight change in other thermodynamic parameters drives the system from one state to the other.

The cell has a very crowded environment and biomolecules remain confined in it. Motivated by this, the static and dynamic properties of biopolymers have been investigated in the confined environment [15–18]. A notable example is translocation, where the geometry of the pore can influence the rate of translocation through the pore. This geometry may be controlled by either choosing different structures of natural nanopores, e.g., alpha-hemolysin (cylindrical pore) or aerolysin (conical pore), or through the construction of artificial pores, which will in general be conical. Most of the theoretical studies have been focused on equilibrium properties of polymers in confined geometry, e.g., slit, cylinder, sphere, cone, etc. [19–25]. These studies revealed that biopolymers under confinement (e.g., proteins in various cavities in the cell or DNA molecules in viral capsids) adopt conformations which are unlikely to occur in the free space [26]. The effects of confinement on the coil-globule transition have also been investigated by varying the width of the slit [19,20] or changing the radius of the cylinder or sphere [21,22]. Although there are studies related to a polymer confined in a wedgelike geometry in a good solvent, to the best of our knowledge, the effect of wedge-shaped geometries on the θ temperature remains unexplored.

It is pertinent to mention here that wedge geometries are quite common in living systems. Unlike the cylinder or slit, in the wedge-shaped geometry the reduction in entropy due to confinement is not a constant but varies as one moves along the conical axis. Such a confined geometry not only reduces entropic contribution but may help in gaining or reducing the enthalpic contribution to the free energy as one moves towards the apex. One of the challenges in polymer translocation experiments is the ability to control the speed of translocation through a biological pore, such as aerolysin, to enable a translation between the electrical signal of charged ions flowing through the pore (which rises or falls depending on the degree to which the polymer blocks the pore) and the details of the translocated protein (see, e.g., Piguet *et al.* [27]). Moreover, from a statistical mechanics perspective, such systems provide a deeper understanding of finite-size effects, which is particularly relevant when a polymer is confined by a nanoscale geometry.

Earlier studies relating to a polymer in good solvent were restricted to the obvious angles for a square lattice, i.e., $\pi/4$, $\pi/2$, π, etc. [23–25]. Here we consider arbitrary angles. For this, we consider n_x bonds along the $\pm x$-direction followed by $+n_y$ (or $-n_y$) bonds in the y direction, and so on. The coordinates (n_x, n_y) correspond to impenetrable reflecting surfaces meeting at the origin having an apex angle 2α, where $\alpha = \tan^{-1}(\frac{n_x}{n_y})$ as shown in Fig. 1(a). Depending on the values of n_x and n_y, one can construct various apex angles ranging from 0° to 180°. One end of the polymer chain is fixed at a distance y from the tip, whereas the other end is left free [Fig. 1(b)].

In the bulk, the typical size of a polymer, either measured by the end-to-end distance or the radius of gyration, scales as $R \sim N^{\nu}$. Here ν is the geometrical exponent corresponding to $1/d_H$, where d_H is the Hausdorff dimension of the walk. In the collapsed state (low temperature or poor solvent) $\nu = 1/d$, while at high temperatures (swollen state) ν is given quite accurately by the Flory approximation $\nu = \frac{3}{(d+2)}$ [28,29]. If the size of the polymer is less than the distance to the cone walls

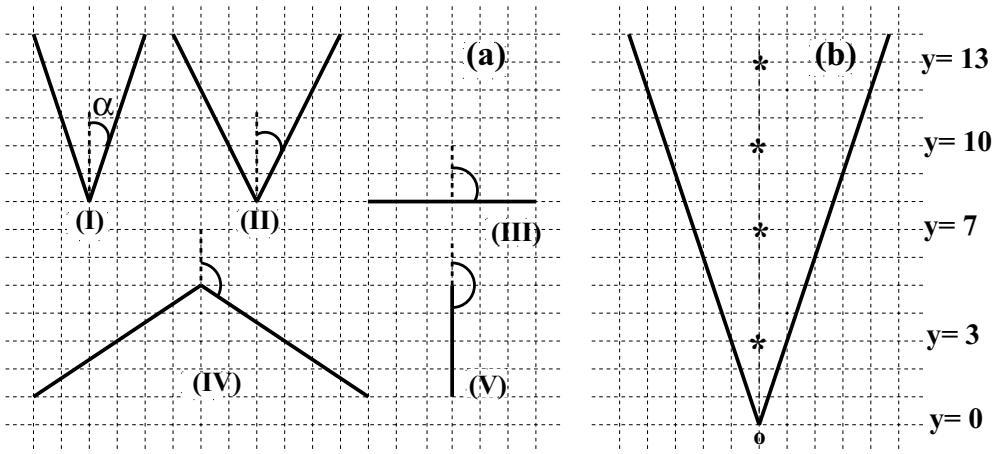

FIG. 1. (a) Schematic representations of different wedge-shaped geometries: (I) $\alpha = 18.43^\circ$, (II) $\alpha = 26.56^\circ$, (III) $\alpha = 90.00^\circ$, (IV) $\alpha = 123.69^\circ$, and (V) $\alpha = 180.0^\circ$. (b) Conical axis marked by $*$ corresponds to the site, where one end of the polymer is anchored, while the other end is free.

from the point where the polymer is anchored, the polymer will not experience any significant confinement. However, if the size of the polymer is greater than this distance, the polymer will experience confinement, which may change its behavior, and is the main focus of the present study.

In statistical mechanical studies of polymers, we are often interested in the infinite chain scaling limit, and indeed the true thermodynamic phase transition occurs strictly in this limit. In reality, even though polymer chains may be very long, but they are invariably of finite length. In this Rapid Communication, we aim to understand the general equilibrium features of a finite chain confined in a cone in a solvent of variable quality, and explore how this may affect its behavior. We also look at the scaling behavior of the chain, and show that many of the qualitative features survive in the scaling limit, and so are true for any polymer of finite length. In what follows, we will refer to the θ temperature for a finite polymer; this is to be understood as the finite-size estimate of the temperature as defined by the peak of the heat capacity C [30], which is expected to diverge in the thermodynamic limit.

We consider a self-attracting–self-avoiding walk (SASAW) model of polymer on a square lattice, which consists of self-avoiding walk configurations with an attractive energy $\varepsilon < 0$ between nonconsecutive, nearest-neighbor, visited lattice sites. We study the equilibrium properties through stochastic enumeration using the Flat-PERM algorithm [31,32] for lengths up to 300 confined to a wedge of angle $\alpha \in [0, \pi]$, as shown in Fig. 1. In previous studies, one end of the polymer is anchored at the origin [23–25]. Here we wish to examine the behavior of the chain and in particular its effect on the θ temperature as it is progressively constrained by the cone. To do this, we consider one end of the polymer anchored along the line of symmetry at a distance y from the apex. In what follows we measure the temperature in units of $|\varepsilon|/k$.

In Fig. 2, we depict the variation in θ temperature with y for different lengths up to $N = 300$ plotted in terms of scaled variables $N^{\phi}|T_\theta - T_c(N)|$ vs y/N^{ν} for $\alpha = 18.43^\circ$ ($n_x = 1$ for every $n_y = 3$ steps in the y direction). $\phi = 3/7$ is the crossover exponent for a two-dimensional SASAW at the θ point, where $\nu = 4/7$ [33]. $T_c(N)$ is the θ temperature corresponding to the length N and T_θ is its value in the thermodynamic limit. This is nonmonotonous with y for all values of N, but can be seen to tend to a constant value, equal to its bulk value, as y becomes large enough. The estimated θ temperature for length $N = 30$ has been found to be ≈ 0.94 [34]. Similar plots for larger N are qualitatively similar, but the finite-size θ temperatures are expected to approach the thermodynamic bulk value ≈ 1.509 [35,36]. The scaled temperature takes into account the anticipated shift in the peak in the heat capacity and the scaled distance measures the distance as a proportion of the gyration radius (up to a scale factor). The curves can be seen to show a good data collapse to one curve, indicating that the general features observed in Fig. 2 subsist for all finite-length chains, even though there is one thermodynamic temperature.

The nonmonotonic (finite-size) behavior of the θ temperature with y gives insight into the behavior of a polymer translocating through a wedge-shaped pore, which is a common geometry both in naturally occurring and man-made nanopores. We consider forced translocation where one end is pulled slowly along the conical axis. In this case, the polymer

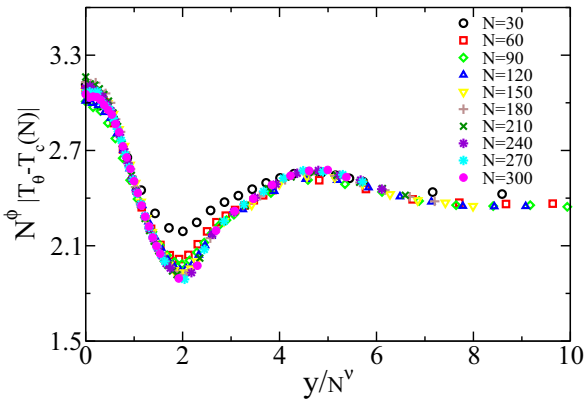

FIG. 2. Variation of scaled temperatures as a function of y/N^{ν} for the apex angle $\alpha = 18.43^\circ$. Note that since we are varying $T_c(N)$, the variation of the curve is opposite to that of the temperature.

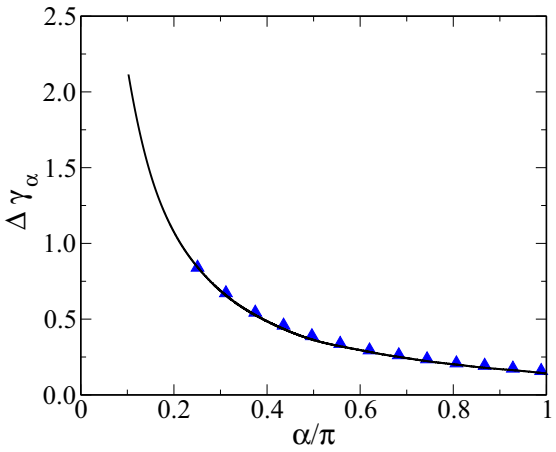

FIG. 3. Curve represents the variation of $\Delta\gamma_\alpha$ as a function of the normalized apex angle. Triangles represent the values obtained from the exact enumeration technique. The solid line is the analytical result proposed in Ref. [23].

will be close to equilibrium at each stage of the translocation process. We can see that it is possible, with suitably tuned parameters, for a collapsed polymer at large y to be in the swollen state as the local θ temperature drops, to recollapse, and then be in swollen state as the polymer reaches the tip. Alternatively, at higher temperatures, the polymer can be made to collapse by bringing it into the pore, but then the chain will be in swollen state again as the polymer tip reaches the apex of the wedge. Perhaps fine-tuning of the solvent quality can be used to accurately control this repeated succession of collapse transitions, in order to slow the passage of the polymer through the pore, a necessary condition for accurate, fast DNA sequencing through translocation.

The results from the stochastic enumeration method are checked using exact enumeration, where results for the small chain can be derived exactly. This lack of simulation errors enables, with the use of suitable extrapolation techniques, one to obtain results in the thermodynamic limit. First, we consider SAW for which exact results are available [23,24]. In free space, the number of configurations C_N of an N-step lattice walk starting from the origin scales as $\approx\mu^N N^{\gamma-1}$. Here, μ represents the connectivity constant of the lattice for the SAWs, and γ is the critical exponent, which depends on the dimensionality d. The statistics of the polymer conformations in the presence of such confining geometry is found to be changed. Using conformal invariance theory, a similar relationship for a linear polymer confined in the wedge-shaped geometry $C_\alpha^N \approx \mu^N N^{\gamma_\alpha-1}$ has been proposed [23,24]. In the presence of a wedge opened at an angle (apex angle) of magnitude α, loss of the conformation is adjusted by γ_α, whereas μ remains almost the same [37]. It is straightforward to have a $\ln(C^N/C_\alpha^N) \sim \Delta\gamma_\alpha \ln N$ relationship, where $\Delta\gamma_\alpha = \gamma - \gamma_\alpha$ is the slope. In Fig. 3, we show the plot of $\Delta\gamma_\alpha$ with α, which is in good agreement with the values predicted in Refs. [23,24]. A slight difference in the value obtained from the exact enumeration technique and the analytical result is due to the nature of the wall. In the present model, walls have been taken as perfectly reflecting, whereas the walker was allowed to visit the walls in Refs. [23,24].

After establishing that exact enumeration can capture the essential physics of SAW in a confined geometry, we now estimate the θ temperature for a finite chain. The partition function of a polymer chain can be expressed as $Z^y(T) = \sum_{N_p} C_N^y(N_p)u^{N_p}$. Here, u corresponds to the Boltzmann weight for the nearest-neighbor interaction. We plot the variation of θ temperature with y in Fig. 4 for two different values α. One of the major advantages of an enumeration technique (exact or stochastic) is that the density of states can be probed to get information of the system at any temperature [38]. The partition function can be expressed in terms of the density of states as $Z^y(T) = \sum_{(N_p)} D(N_p)$, where $D(N_p) = C_N^y(N_p)u^{N_p}$ is the weighted density of states, which contains all information on energetic quantities of a statistical system. In order to explore the origin of the nonmonotonic behavior of θ temperature, we have plotted $D(N_p)$ as a function of N_p at the θ temperature for the angle $\alpha = 26.56^\circ$ in Figs. 5(a)–5(c). The plots are for a walk of length 30 and are calculated using exact enumeration, to avoid any statistical errors inherent with the Flat-PERM.

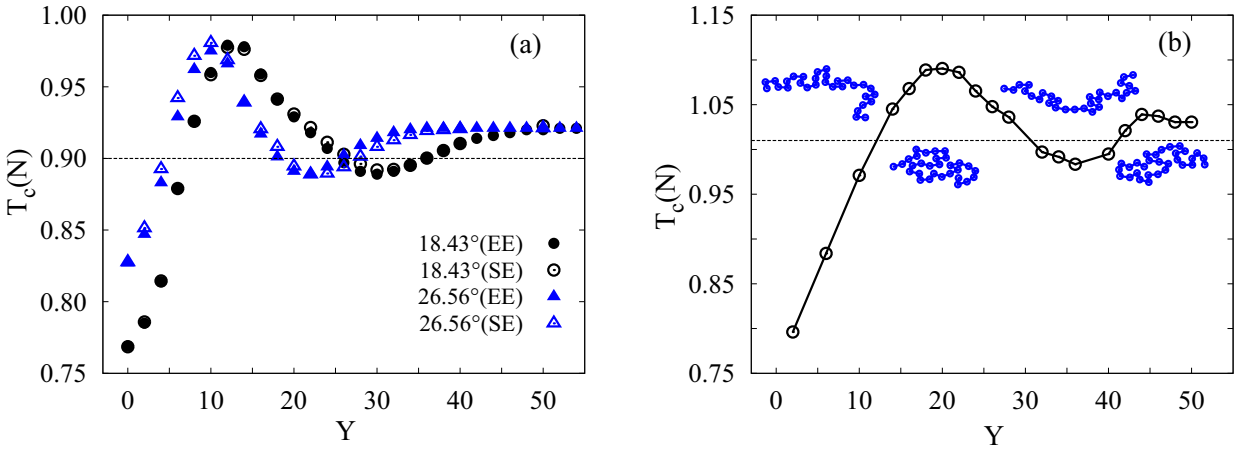

FIG. 4. (a) shows the θ-temperature profile of a polymer chain $N = 30$, whose starting points have been varied systematically from $y = 50$ to 0 for different apex angles. Solid and open symbols are data obtained from exact and stochastic enumeration, respectively. (b) shows the corresponding result for $\alpha = 18$, obtained from the Langevin dynamics simulations with snapshots of that region.

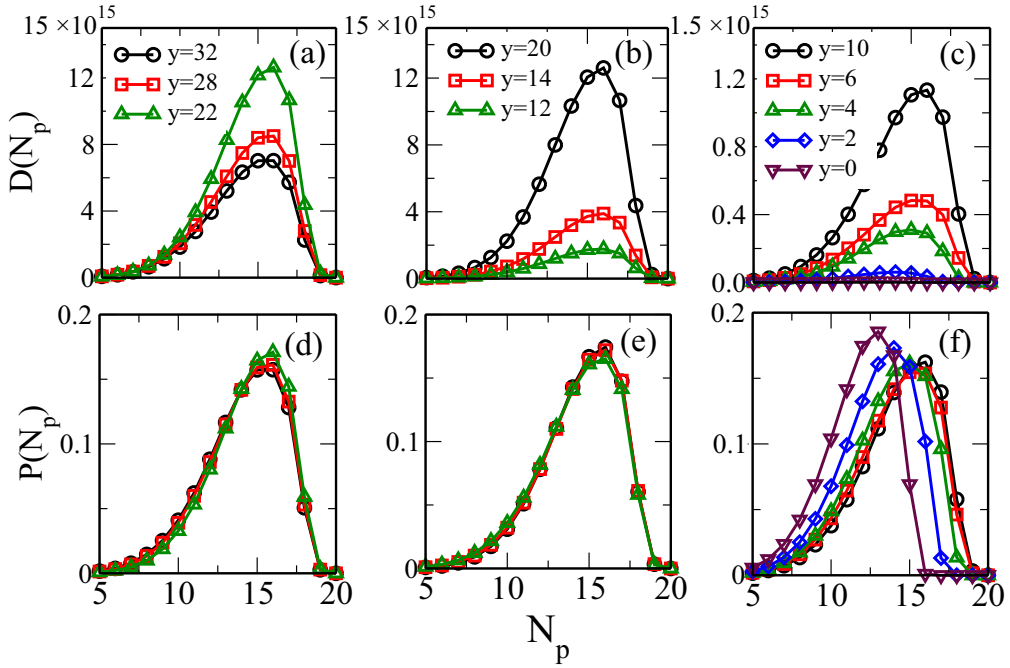

FIG. 5. (a)–(c) show the weighted density of states as a function of N_p at fixed apex angle 26.56°. (a) for a region $y = 32 - 22$, one can see an increase in entropy, which leads to a decrease in the θ temperature (Fig. 4). (b) In the region $y = 20$ to $= 12$, entropy decreases which results in an increase in temperature. (c) From $y = 10$ to the origin, the peak value occurs at different N_p, which corresponds to a decrease in enthalpy, and thus one observes the sharp fall in the θ temperature. (d)–(f) have been scaled with corresponding $C_N(N_p)$ to show the shift in peak positions.

The most dominant contribution to the partition function or the free energy $[-T \ln Z^y(T)]$ is from the peak value of $D(N_p)$ (Fig. 5). It is apparent from Fig. 4 that when the starting point moves towards the origin (up to $y = 32$), the θ temperature remains constant and the system exhibits the bulk behavior. In the range $y = 32$–22, there is a decrease in the θ temperature (Fig. 4). This can be attributed to the gain in entropy, which can be seen from Fig. 5(a), where the peak value of the most dominant term is increasing as y moves from $32 \rightarrow 22$, whereas the peak position remains constant. It is important to realize here that the total free energy of the system is changing as the number of conformations contributing to the partition function is decreasing because of the confinement as one moves towards the origin.

In the range $y = 20$–12, one observes in Fig. 4 that the θ temperature is increasing. This is because of the decrease in the peak value of the dominating term [Fig. 5(b)]. Interestingly, in this region the peak position also remains constant. In fact, in this region the shape of the polymer gets deformed due to the confinement though the value of N_P remains almost the same. $y = 10$–0 corresponds to the maximum confinement on the polymer. In this region, polymer can visit less number of sites, which inhibits the formation of the contact. As a result, the value of N_p decreases, and a fraction of the chain is forced to be in the extended state. This can be seen from Fig. 5(c), where the peak position shifts towards the lower value of N_p. This causes a net decrease in enthalpy. As a result, the θ temperature decreases sharply. In fact the complete $\theta - y$ profile is an interplay between enthalpy and entropy, which could be visualized by analyzing the density of states.

The consequences of confinement arising due to the different values of α are another striking result shown in Fig. 4. It can be seen from the plot that the θ temperature for the $\alpha = 26.56°$ in the region $y = 45$–25 is higher than the $\alpha = 18.43°$. However, in the region $y = 25$–10, the θ temperature for the $\alpha = 18.43°$ is higher than the $\alpha = 26.56°$. Interestingly, in the range $y = 10$–0, the θ temperature for the $\alpha = 26.56°$ is found to be higher than the $\alpha = 18.43°$. The mismatch between the maxima and minima at different angles would enable the passage from swollen to collapsed by changing the apex angle α, which may be used in designing molecular gate or switch, where instead of varying the temperature or the quality of solvent, a polymer chain may be brought to the collapsed state from the swollen state or *vice versa* by varying the confinement. Such behavior may be important in biological processes, e.g., transport of biomolecules from one region to the other at a constant temperature, where an energy barrier may hinder the transport. Such energy barrier may be overcome by varying the confinement and lead progressive movement of biomolecules from one region to the other.

To understand the appearance of free-energy barriers as a result of geometry is important in a number of nanotechnological applications and in the understanding of the functioning of biological systems. The scaling behavior of the system provides a deeper insight. The details will be presented elsewhere [39]. The use of exact and stochastic enumeration together appeared to be a very useful tool, as in one case the coefficients of the partition function are exactly known, while in the other they can be extended approximately (but to good accuracy) for longer chains, enabling the thermodynamic limit

to be more easily probed. In order to rule out that this is an artifact of the lattice model, we performed off-lattice Langevin dynamics simulation of a coarse-grained model of polymer [40]. The details of the force field and simulations are described in the Supplemental Material [31]. The variation of θ temperature with y is shown in the lower plot in Fig. 4, which is qualitatively similar to the one obtained through either stochastic or exact enumeration. This gives unequivocal support for the existence of nonmonotonic behavior in real systems; therefore, at this stage our studies call for further experiments on the coil-globule transition in such confining geometries.

Financial assistance from the SERB, SPARC, MHRD, and UGC, India is gratefully acknowledged. K.C. and S.S. would like to thank DST-INSPIRE, India. S.K. would like to acknowledge ICTP, Italy, where a part of the work has been carried out.

[1] A. I. Zotin, *Thermodynamic Bases of Biological Processes Physiological Reactions and Adaptions* (Walter de Gruyter, Berlin, 1990).
[2] C. Duan, W. Wang, and Q. Xie, Biomicrofluidics **7**, 026501 (2013).
[3] F. Wagner, G. Lattanzi, and E. Frey, Phys. Rev. E **75**, 050902(R) (2007).
[4] W. Reisner, J. N. Pedersen, and R. H. Austin, Rep. Prog. Phys. **75**, 106601 (2012).
[5] P. Doty, J. Marmur, J. Eigner, and C. Schildkraut, Proc. Natl. Acad. Sci. U.S.A. **46**, 461 (1960).
[6] M. Rief, M. Gautel, F. Oesterhelt, J. M. Fernandez, and H. E. Gaub, Science **276**, 1109 (1997).
[7] M. Cieplak, T. X. Hoang, and M. S. Li, Phys. Rev. Lett. **83**, 1684 (1999).
[8] U. Bockelmann, B. Essevaz-Roulet, and F. Heslot, Phys. Rev. Lett. **79**, 4489 (1997).
[9] C. Danilowicz, Y. Kafri, R. S. Conroy, V. W. Coljee, J. Weeks, and M. Prentiss, Phys. Rev. Lett. **93**, 078101 (2004).
[10] D. Marenduzzo, S. M. Bhattacharjee, A. Maritan, E. Orlandini, and F. Seno, Phys. Rev. Lett. **88**, 028102 (2001).
[11] S. Kumar and G. Mishra, Phys. Rev. Lett. **110**, 258102 (2013).
[12] M. Wartell and A. S. Benight, Phys. Rep. **126**, 67 (1985).
[13] P. G. de Gennes, J. Physique Lett. **36**, 55 (1975).
[14] M. Muthukumar, *Polymer Translocation* (CRC, Boca Raton, FL, 2011).
[15] A. P. Minton, J. Biol. Chem. **276**, 10577 (2001).
[16] M. S. Cheung, D. Klinov, and D. Thirumalai, Proc. Natl. Acad. Sci. U.S.A. **102**, 4753 (2005).
[17] A. R. Singh, D. Giri, and S. Kumar, Phys. Rev. E **79**, 051801 (2009).
[18] D. Marenduzzo, C. Micheletti, and E. Orlandini, J. Phys.: Condens. Matter **22**, 283102 (2010).
[19] J. Tang, S. L. Levy, D. W. Trahan, J. J. Jones, H. G. Craighead, and P. S. Doyle, Macromolecules **43**, 7368 (2010).
[20] L. Dai, C. B. Renner, J. Yan, and P. S. Doyle, Sci. Rep. **5**, 18438 (2015).
[21] W. Reisner, K. J. Morton, R. Riehn, Y. M. Wang, Z. Yu, M. Rosen, J. C. Sturm, S. Y. Chou, E. Frey, and R. H. Austin, Phys. Rev. Lett. **94**, 196101 (2005).
[22] P. Cifra and T. Bleha, Macromol. Theory Simul. **21**, 15 (2012).
[23] J. L. Cardy and S. Redner, J. Phys. A: Math. Gen. **17**, L933 (1984).
[24] A. J. Guttmann and G. M. Torrie, J. Phys. A **17**, 3539 (1984).
[25] Y. Hammer and Y. Kantor, Phys. Rev. E **89**, 022601 (2014).
[26] Y. Liu and B. Chakraborty, Phys. Biol. **5**, 026004 (2008).
[27] F. Piguet, H. Ouldali, M. Pastoriza-Gallego, P. Manivet, J. Pelta, and A. Oukhaled, Nat. Commun. **9**, 966 (2018).
[28] P. G. de Gennes, *Scaling Concepts in Polymer Physics* (Cornell University Press, Ithaca, 1979).
[29] C. Vanderzande, *Lattice Models of Polymers* (Cambridge University Press, Cambridge, 1998).
[30] Increase in the peak height of the specific heat with N is being considered as indicative of a phase transition, especially when the system size is small.
[31] See Supplemental Material at http://link.aps.org/supplemental/10.1103/PhysRevE.101.030502 for details of Langevin dynamics simulation.
[32] T. Prellberg and J. Krawczyk, Phys. Rev. Lett. **92**, 120602 (2004).
[33] B. Duplantier and H. Saleur, Phys. Rev. Lett. **59**, 539 (1987).
[34] S. Kumar and D. Giri, Phys. Rev. E **72**, 052901 (2005).
[35] D. P. Foster, E. Orlandini, and M. C. Tesi, J. Phys. A **25**, L1211 (1992).
[36] S. Kumar, I. Jensen, J. L. Jacobsen, and A. J. Guttmann, Phys. Rev. Lett. **98**, 128101 (2007).
[37] S. G. Whittington, J. Chem. Phys. **63**, 779 (1975).
[38] M. Bachmann and W. Janke, Acta Phys. Pol. B **34**, 4689 (2003).
[39] K. Chauhan, D. P. Foster, and S. Kumar (unpublished).
[40] D. Frenkel and B. Smith, *Understanding Molecular Simulation* (Academic, San Diego, 2002).